ACS OMEGA

http://pubs.acs.org/journal/acsodf

Article

Mechanical Reinforcement of Lamellar Bilayer Hydrogels by Small Amounts of Co-surfactants

Milena Lama and Jian Ping Gong*

Cite This: *ACS Omega* 2023, 8, 25185−25194

Read Online

ACCESS | Metrics & More | Article Recommendations | Supporting Information

ABSTRACT: Anisotropic photonic hydrogels with alternatively stacked poly(dodecyl glyceryl itaconate) (PDGI) bilayers and polyacrylamide (PAAm) gel layers are unique soft materials with various functions. It is known that to form the lamellar phase of bilayers, a small amount of co-surfactant sodium dodecyl sulfate (SDS) should be present in the precursor monomer solutions of the gels. However, little is known about the influence of the co-surfactant on the structure of bilayers and on the mechanical properties of such photonic hydrogels. Herein, we chose several co-surfactants and studied the effect of the co-surfactants on the self-assembly behavior of the bilayers and on the mechanical properties of the resulting photonic hydrogels. A macroscopically aligned lamellar phase could be induced for all the co-surfactants. Interestingly, the mechanical response of the photonic hydrogels sensitively depends on the chemical structure of the co-surfactant, especially at large deformation. We hypothesize that doping by small amounts of co-surfactants dramatically changes the anchoring strength and density of PAAm strands onto the bilayer surface, thereby influencing the load transfer efficiency from the bilayer to the PAAm gel layer at large deformation and the rupture of the bilayer. This work provides new understanding in the molecular mechanisms of deformation and strengthening in this soft and anisotropic nanocomposite, helping to design more robust photonic hydrogels.

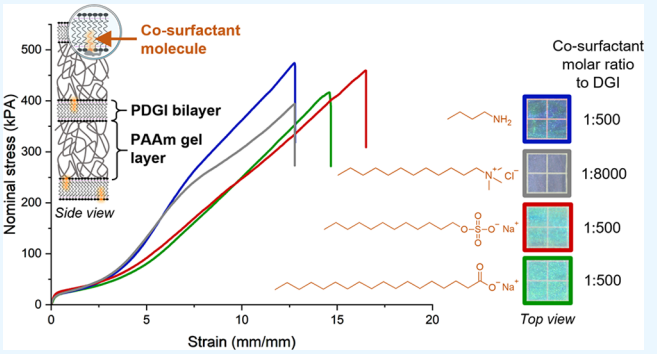

INTRODUCTION

Under certain conditions, surfactants are known to form different structures in aqueous solution through self-assembly,[1] e.g., micellar and lamellar. Such organizations rely on a critical packing parameter[2] defined by the ratio between the volume occupied by the hydrophobic tail on the one hand and the product between the surface area of the hydrophilic head and the length of the hydrophobic tail on the other hand. These geometrical parameters depend on the chemical structure of the surfactant including ionic and non-ionic but can also be tuned to some extent by the physico-chemical environment, e.g., pH, temperature, or doping by co-surfactants in small quantities.[3,4] Very small amounts of sodium dodecyl sulfate (SDS), a widely used anionic surfactant, were found to enable the non-ionic surfactants to form lamellar phases.[5,6] By doping in non-ionic amphiphiles, SDS prevents phase segregation in aqueous solution by lowering the energy of the system. Moreover, SDS plays a role as a stabilizer in the case of defects in lamellar organizations (such defects are inherent to liquid crystalline organizations[7]), thus increasing the lifetime of the assemblies. In this work, we chose monomeric dodecylglyceryl itaconate (DGI) as a non-ionic surfactant. DGI molecules alone phase-separate into micelles in water. In the presence of small amounts of the co-surfactant SDS, DGI molecules form lamellar liquid crystal phases above the Krafft point of DGI (43 °C), exhibiting iridescent color. The color of such solutions depends on the SDS concentration relative to DGI.[8] Specifically, the solution is red at low SDS content (0.025 mol % of DGI) and undergoes a blue-shift at higher SDS concentrations (2.5 mol % of DGI). Indeed, SDS enables to reduce the distance between neighboring lamellae and compensates the appearance of subsequent defects as mentioned above.

Tsujii and co-workers immobilized the lamellar liquid crystal phases of monomeric DGI in the chemically crosslinked polyacrylamide (PAAm) network through one-pot polymerization of the DGI monomer and acrylamide monomer. They found that DGI and AAm are independently polymerized and the polymeric DGI (PDGI) bilayers are embedded in the PAAm gel matrix physically without covalent bonding between the two networks.[9] By applying shear to the precursor monomer solution, Haque and co-workers succeeded in

Received: April 4, 2023
Accepted: June 13, 2023
Published: July 3, 2023

synthesizing hydrogels with uniaxially aligned bilayers.[10−13] These PDGI/PAAm hydrogels showed unique properties, such as one-dimensional swelling, tunable structural colors, and anisotropic mechanical properties. The adsorption of the PAAm gel phase onto PDGI bilayers through strong hydrogen bonding[14] endows the photonic hydrogels with high strength and toughness. Although Tsujii and co-workers initially reported the possible use of different co-surfactants to obtain iridescent DGI solutions,[6] solely SDS at fixed amounts relative to DGI (0.025 mol % of DGI) has been used so far in the studies of PDGI/PAAm hydrogels. Therefore, the influence of co-surfactants on the self-assembly of DGI and on the properties of PDGI/PAAm hydrogels remains poorly understood.

Herein, we report the effect of different co-surfactants on the formation of lamellar liquid crystal phases of DGI and on the mechanical properties of PDGI/PAAm hydrogels as composite materials. We first investigated in which concentration range these co-surfactants allow to form uniaxially aligned bilayers in the PDGI/PAAm hydrogels. Then, we studied the mechanical behavior of the PDGI/PAAm hydrogels by tensile tests at the equilibrium swelling state. USAXS analysis enabled to unravel the structure change at large deformation. By comparing with the behavior at the as-prepared state, we hypothesize on the possible mechanisms induced by different co-surfactants.

EXPERIMENTAL SECTION

Materials. Dodecylglyceryl itaconate (DGI) as an amphiphilic monomer was synthesized from scratch as described elsewhere.[6] The crude product was purified by silica gel column chromatography with a mixture of hexane and ethyl acetate as the eluant (1:1 by volume). The obtained product was further recrystallized twice from an acetone/hexane mixture (1:1 by weight). Acrylamide (AAm) (Wako) as the monomer was recrystallized from chloroform and *N*,*N*′-methylenebisacrylamide (MBAA) (Wako) as the crosslinker was recrystallized from ethanol. Irgacure 2959 (Wako) as the initiator and SDS (Wako), sodium stearate (SST) (Wako), dodecyltriethylamine chloride (DTAC) (Wako), N-butylamine (NBA) (Wako) as co-surfactants were used as received. MilliQ water was used to prepare the precursor solutions and swell the hydrogels. Paraffin oil (Wako) was used to preserve the hydrogels at the prepared state in order to prevent any swelling or dehydration.

Synthesis of Uniaxially Aligned Lamellar PDGI/PAAm Hydrogels with Various Co-surfactants. PDGI/PAAm hydrogels with different co-surfactants were synthesized by simultaneous free radical polymerization from aqueous solutions containing 0.1 M DGI, prescribed amounts of co-surfactants, 2 M AAm, 2 mM MBAA, and 2 mM Irgacure 2959, following the same procedure as described elsewhere.[10,15] Briefly, the precursor solutions were introduced into a glass vial, which was heated at 55 °C (above the Krafft point of DGI at 43 °C) in a water bath for 5−6 h to induce the self-assembly of DGI in its lamellar phase. After removing the dissolved oxygen in an argon glovebox, the transparent blueish solution was manually sucked through a rectangular mold by a syringe connected to polyethylene tubing. The rectangular mold was made from two parallel glass plates separated by a 0.5 mm thick silicone spacer. This sucking process applied a shear to the solution and enabled to align lamellar bilayers along the glass sheet surfaces. Then, samples were kept for overnight UV polymerization in an oven at 38 °C to avoid over-heating from UV light. As control samples, PAAm hydrogels with co-surfactants (SDS or NBA at R = 1:250) were synthesized by the exact same procedure but without DGI. After polymerization, hydrogels of sheet shape were either directly placed in paraffin oil (as-prepared state) or swollen in MilliQ water for at least 7 days to reach the equilibrium swelling state.

Swelling Ratios. To characterize the anisotropic structure of the hydrogels, equilibrium swelling ratios in MilliQ water were measured in the thickness direction and in width and length directions, at room temperature. The thickness of the hydrogels was measured by means of a thickness meter or a caliper. The length and width of the gels were measured from photographs post-treated by ImageJ software. The swelling ratios were relative to the as-prepared state. Three samples per condition were averaged, except for the gel with DTAC concentration at 0.05 mol % of DGI because the precursor solution was already slightly opaque (no proper self-assembly into lamellar bilayers).

Reflection Spectra. The layered structure of PDGI/PAAm hydrogels acts as a Bragg's mirror and is at the origin of the photonic properties of the hydrogels.[11] To characterize the lamellar structure, reflectance properties of the hydrogels were measured at room temperature using a white light source (Xe lamp), a variable angle light detector (Hamamatsu Photonics KK, C10027A10687), and a photonic multichannel analyzer (Hamamatsu Photonics KK, C10027). The reflectance was obtained by fixing the incident angle at 60° and the reflection angle at 45°. The curves were smoothened using Origin software. The interlamellar distance d was calculated using Bragg's law of diffraction $2nd\sin(\theta) = \lambda_{max,}$[8] where n = 1.33 is the refractive index of water, θ is the angle of incidence, and λ_{max} is the wavelength at maximum reflectance intensity.

Cryo-scanning Electron Microscopy (Cryo-SEM). Cryo-scanning electron microscopy was used to characterize the microstructure. Hydrogels were cut at room temperature in 6 mm width and 2.5 mm high strips and then sandwiched between two copper plates in the sample holder. Cryogenic glue was applied at the bottom of the sample holder to fix the sample. The sample holder was then immersed for a couple of minutes in liquid nitrogen under vacuum (flash-freezing) and then was quickly placed inside the preparation chamber of the microscope (under vacuum, at −150 °C). The upper part of the sample which exceeds the sample holder's height was removed by cutting horizontally with a surgical blade to minimize observation artifacts. Indeed, sample exceeding the height of the sample holder will undergo slightly lower freezing speed due to the absence of full contact with a conductive surface that could induce the formation of ice crystals, thus disrupting the original structure. The surface of the sample was then etched for 10 min at −95 °C before being coated by a 10 nm layer of gold. Observations were performed on a JEOL JSM-6710F high resolution scanning electron microscope equipped with a Gatan ALTO2500 cryo-unit at an acceleration voltage of 3 kV.

Mechanical Tests. Uniaxial tensile and cyclic tensile tests were performed to measure the mechanical properties of the hydrogels. The sheet shaped samples were cut into a standardized dumbbell shape by a gel cutter (JIS-6251-7, gauge length 20 mm, gauge width 4 mm for uniaxial tensile tests and gauge length 12 mm, gauge width 2 mm for cyclic tests). Uniaxial tensile tests were carried out on an Instron tensile tester model 5965, equipped with pneumatic clamps

https://doi.org/10.1021/acsomega.3c02274
ACS Omega 2023, 8, 25185−25194

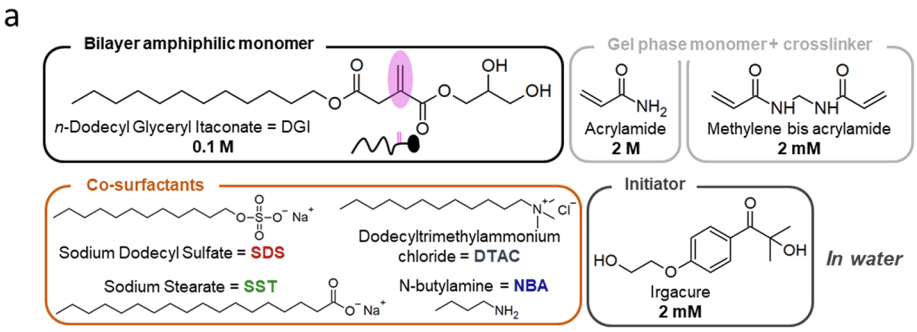

b

Surfactant	Headgroup area, a_0 (nm²)	Hydrophobic tail length, l_t (carbon atoms)
DGI	*0.3*	*12*
NBA	0.04	4
DTAC	0.14	12
SDS	0.57	12
SST	0.3	17

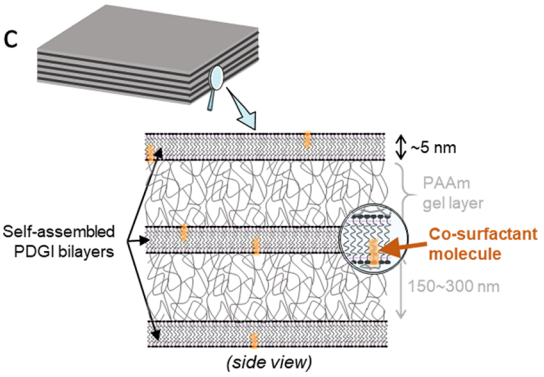

Figure 1. (a) Chemical structures of molecules used in this work. (b) Summary of the geometrical characteristics of monomeric DGI and the four co-surfactants used in this study. Headgroup areas in water were calculated or taken from the literature.[16−18] (c) Illustration of the 1D photonic lamellar structure of PDGI/PAAm hydrogels synthesized by one-pot polymerization of self-assembled monomeric DGI bilayers in PAAm hydrogel precursor solutions. Small amounts of co-surfactants were added to the solutions.

covered with a coarse sandpaper to prevent sample slippage, at a velocity of 100 mm/min. In the case of samples preserved in water, a humidifier was used to prevent sample drying during the test. Cyclic tensile tests were carried out on a tensile-compressive tester (Tensilon RTC-1310A, Orientec Co.) at a velocity of 100 mm/min, in a temperature-controlled water bath filled with MilliQ water to prevent dehydration. Samples were stretched 5 times up to 833% deformation (maximum condition) and down to 0.002 N (minimum condition). Strain was calculated from the displacement of the cross-head. Young's modulus was calculated from the first 10% of the stress−strain curves. Reproducibility was assessed during tensile testing (Three samples from three different hydrogels under the same conditions) and was found to be very high. Two samples per condition were used for cyclic tensile tests and uniaxial tensile tests in the as-prepared state.

Ultra-small Angle X-ray Scattering (USAXS). USAXS measurements of PDGI/PAAm hydrogels were performed at the Spring-8 synchrotron radiation facility (JASRI, Hyogo, Japan), using the beamline BL19B2. The sample-to-detector distance was 42.64 m, and the X-ray wavelength was 0.0517 nm. The intensity was 24 keV. The elongation axis was set vertical to the equatorial direction. The sample (width: 2 mm, length between clamps: 10 mm, thickness ∼1 mm) was fixed in the clamps of a computer-controlled tensile deformation stage (LinKam, model 10073A). The stage was placed in order to stretch the sample vertically in the X-ray irradiation setup. The sample was oriented with its lamellar plane perpendicular to X-ray. A first acquisition was performed at strain = 0 (no stretching). Then, the sample was stretched to strain = 7.3 for another acquisition. During X-ray exposure, the sample was held at constant strain. The X-ray exposure time was 60 s at each strain. The backscattering 2D patterns were recorded on an imaging camera. The 2D image was converted to 1D data using a reduction package Red2D (https://github.com/hurxl/Red2D) on the data analysis software Igor Pro.

RESULTS AND DISCUSSION

Structure of PDGI/PAAm Hydrogels with Different Co-surfactants. The chemical structure of co-surfactants studied in this work is shown in Figure 1a. Geometrical parameters of the co-surfactants, that is, headgroup area a_0 and length of their hydrophobic tail in terms of carbon atom number l_t, are displayed in Figure 1b, along with the data of DGI. SDS and SST are anionic, DTAC is cationic, and they are fully dissociated in water. The pK_a of NBA is around ∼10, meaning that its headgroup is slightly protonated in MilliQ water. Compared to DGI, SDS has the same tail length but its headgroup area is larger, SST has the same headgroup area but a longer tail, and DTAC has a smaller headgroup but the same tail length, while NBA has both smaller headgroup area and shorter tail. In order to investigate the concentration range of each co-surfactant for the formation of the lamellar phase of DGI bilayers, the co-surfactant to DGI molar ratio R was varied in the range R = 1:8000 to 1:64 and other formulations for hydrogel synthesis were fixed (Figure 1a). When uniaxially aligned bilayers are formed in the PDGI/PAAm hydrogels (Figure 1c), the hydrogels should show swelling only in the thickness direction, perpendicular to the bilayers. This is because the alternatively stacked PDGI bilayers are impermeable to water, and swelling is only allowed in the thickness direction of the PAAm gel layers between the bilayers.[10] Thus, characterizing the swelling ratios of the hydrogels in the three directions (length, width, and thickness) specifies the structure of the bilayers.

https://doi.org/10.1021/acsomega.3c02274
ACS Omega 2023, 8, 25185−25194

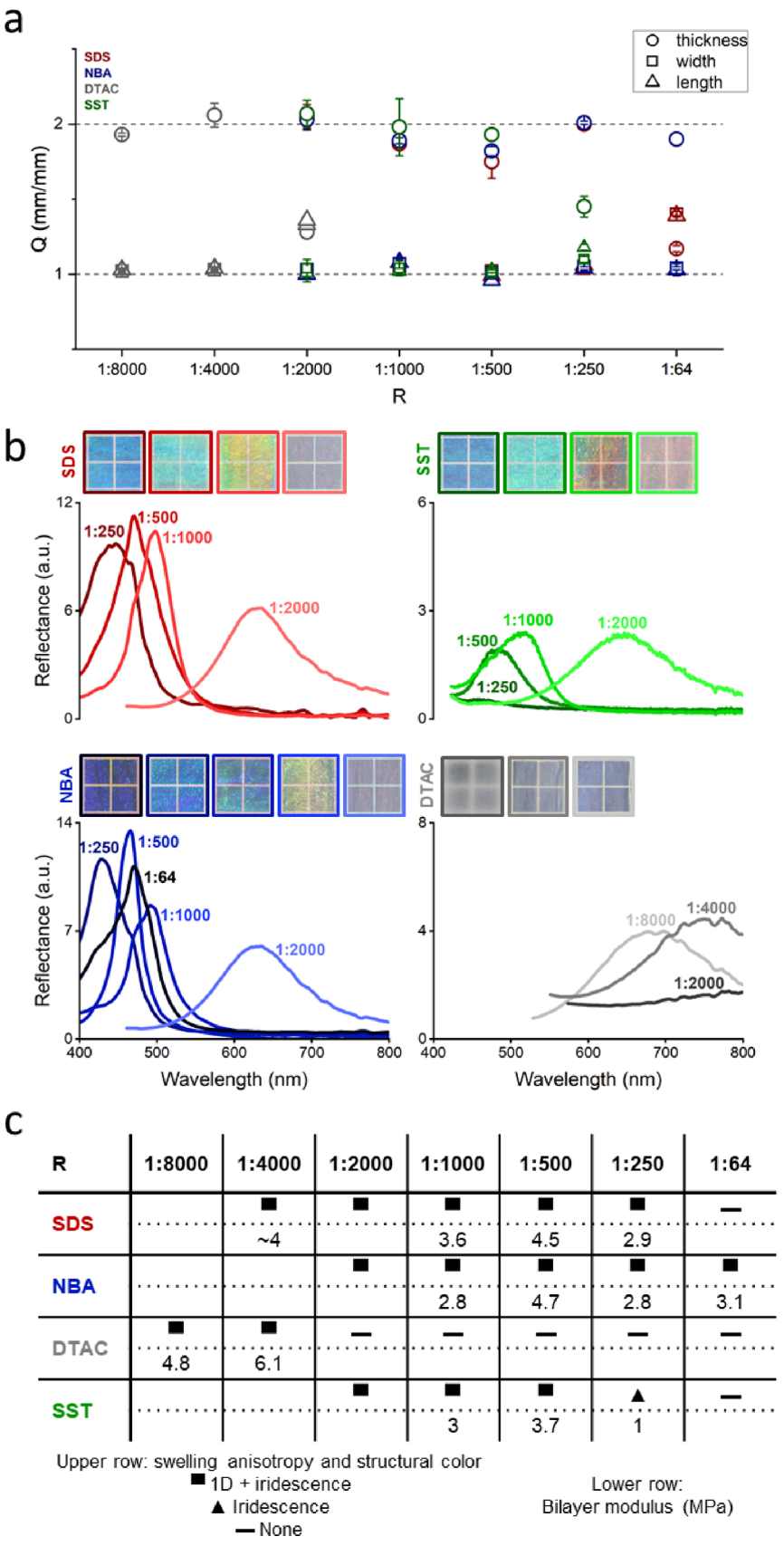

Figure 2. Structure characterization of the PDGI/PAAm hydrogels prepared with different co-surfactant to DGI molar ratio R for the four co-surfactants. (a) Swelling ratios in thickness, width, and length direction relative to the as-prepared state. (b) Photographs of the hydrogels placed on a black substrate (each square of the photos is 5 mm × 5 mm), with increasing *R* from left to right, together with reflectance intensity spectra of the hydrogels. (c) Table summarizing the structural properties of the hydrogels. Upper row: 1D swelling and iridescence properties; lower row: bilayer modulus in MPa estimated from Equation (1) (see Figure S5). The data of SDS at *R* = 1:4000 is from the literature.[10]

https://doi.org/10.1021/acsomega.3c02274
ACS Omega 2023, 8, 25185−25194

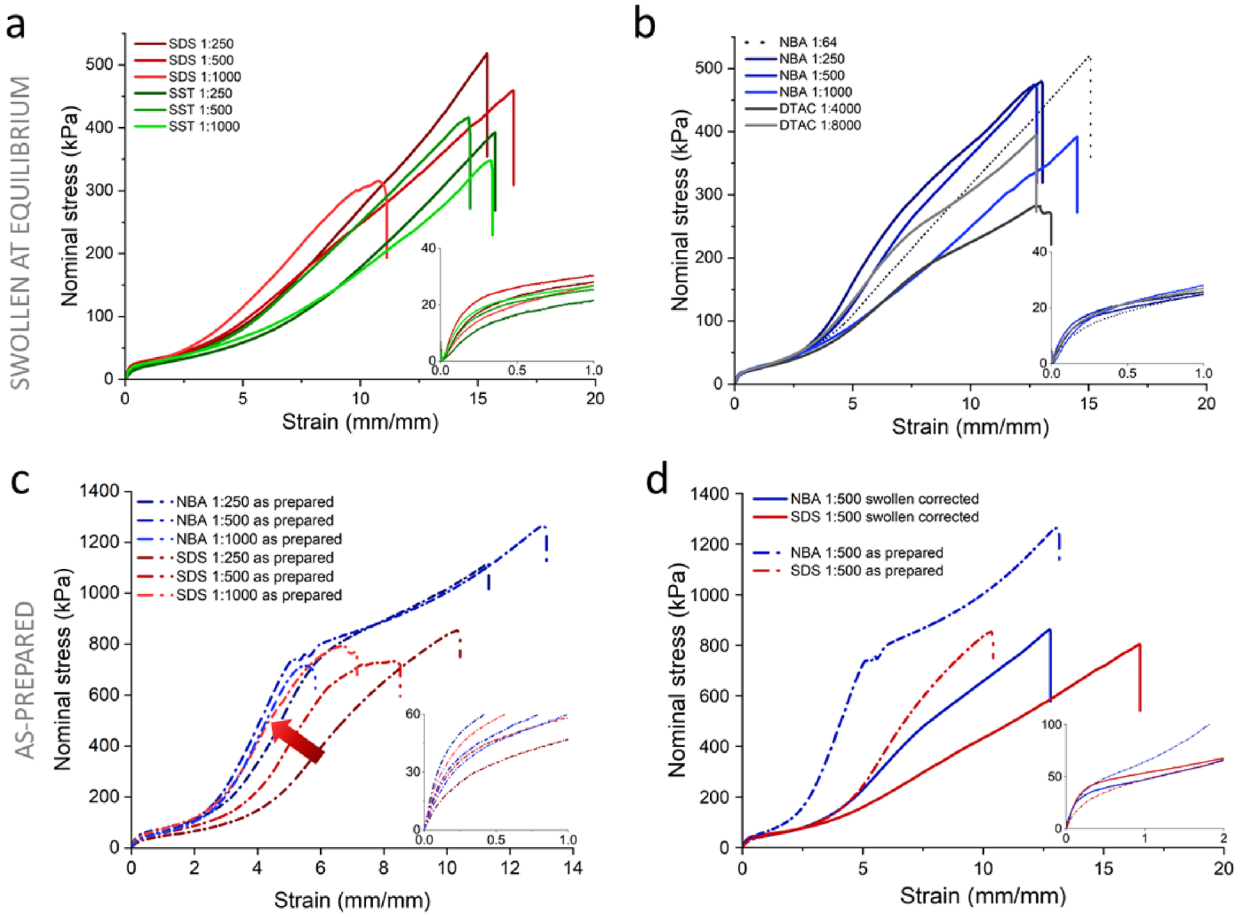

Figure 3. Tensile behavior of PDGI/PAAm hydrogels with uniaxially aligned layered structure prepared with various co-surfactants. (a and b) Representative tensile behavior of the hydrogels at equilibrium swelling. (c) Tensile behavior of hydrogels with SDS or NBA at the as-prepared state, as typical examples. (d) Comparison between the tensile behavior at the as-prepared state and that at the equilibrium swelling state, where the nominal stress for the swollen samples was corrected by their thickness swelling ratio. The tensile response was obtained along the bilayer direction. The numbers in the figures indicate the co-surfactant to DGI molar ratio (R). The insets in each figure show the enlarged plot at small strain.

As plotted in Figure 2a, the hydrogels exhibited one-dimensional swelling behavior at low co-surfactant concentration but lateral swelling occurred at increased co-surfactant concentration, except for NBA. The concentration up to which the 1D swelling was maintained depends on the chemical structure of co-surfactants: for SDS up to R = 1:250, for SST up to R = 1:500, for DTAC up to R = 1:4000, while NBA exhibited one-dimensional swelling even at the highest concentration investigated (R = 1:64). For PDGI/PAAm hydrogels exhibiting 1D swelling, the bilayers are uniaxially aligned in a continuous phase to a macroscopic scale of several centimeters (sample size). However, it is worth mentioning that at the highest NBA concentration (R = 1:64), both uniaxially aligned and curved bilayers were observed in the sample by cryo-SEM (Figure S1). Therefore, according to the structure of the co-surfactant, there is a concentration threshold above which the lamellar bilayer structure is disrupted, which allows 3D swelling. This is consistent with macroscopic observations of iridescence in Figure 2c. When the co-surfactant concentration increases, self-assembled DGI structures would tend to deviate from lamellar to curved ones (hexagonal, micellar) due to increased head-to-head repulsion, especially for charged co-surfactants. Thus, more defects will be induced at increased co-surfactant concentration. Specifically, it was recently shown that swelling PDGI/PAAm hydrogels in SDS solution tend to transform the lamellar bilayers into micelles (above the critical micellar concentration of SDS), which is accompanied by 3D swelling.[19] In our case, since DGI monomers are initially not polymerized when self-assembled in the presence of SDS, a much lower SDS concentration is likely to disturb the lamellae.

We then characterized the structural color to clarify the lamellar structure of the hydrogels. Figure 2b shows photographs of the hydrogels prepared at various R for the four co-surfactants, together with reflectance intensity spectra. In general, hydrogels with SDS, SST, and NBA were transparent, showing bright structural color especially above R = 1:1000, while those with DTAC were slightly opaque, showing dim structural color. Above R = 1:1000, hydrogels with SDS and NBA exhibited reflectance peaks around 400∼500 nm, while the reflectance peaks of hydrogels with SST and DTAC were much weaker. Specifically, hydrogels with DTAC showed peaks in the near-infrared region (around 700∼800 nm), indicating large inter-bilayer spacing d, consistent with their low co-surfactant content. The peaks of hydrogels with SDS, NBA, and SST exhibited a slight blue-shift with increasing amounts of co-surfactants (Figure S2), corresponding to a decrease in the inter-bilayer distance d (Figure S3), in accordance with previous observations for DGI in solution with SDS.[8] In contrast, hydrogels with DTAC showed a slight

https://doi.org/10.1021/acsomega.3c02274
ACS Omega 2023, 8, 25185−25194

red-shift with DTAC concentration increase. Interestingly, the hydrogel with NBA at R = 1:64 exhibited a broader peak, confirming its structural inhomogeneity at large scale. The effect of co-surfactant concentration on anisotropic swelling and structural color is summarized in Figure 2c. For all co-surfactants considered, small R induces both 1D swelling and iridescence, that is, formation of continuous bilayers. However, differences appear at higher R, which depend on the chemical structure of the co-surfactant. For example, the hydrogel with SDS at R = 1:64 was very soft and almost colorless, while some hydrogels exhibited structural color at high R even with an imperfect 1D swelling. Specifically, for SST at R = 1:250, the hydrogel showed lateral swelling and was much softer but exhibited a slightly blueish structural color, meaning that the hydrogel has discontinuous bilayers.[13,19] This observation indicates that a longer hydrophobic tail destabilizes the bilayers, which is also noticed in other liquid crystals.[20] Our work further suggests that in the case of a long hydrophobic tail, a larger headgroup area of the co-surfactant would counter-balance the destabilizing effect. For example, 1D swelling is obtained with DTAC or SDS at R = 1:4000 but not with DTAC at higher R. When the hydrophobic tail is short enough as in the case of NBA, the co-surfactant stabilizes the bilayers over a wider range of concentrations even though the headgroup area is small.

Effect of Co-surfactant Concentration and Swelling on the Mechanical Behavior of the Photonic Hydrogels. To characterize the mechanical properties of the hydrogels, we chose to compare hydrogels with SDS, NBA, and SST above R = 1:1000 and DTAC at R = 1:8000 and 1:4000 since these hydrogels used DGI synthesized from the same batch. In fact, previous work noticed slight variation in tensile behavior of the hydrogels at large deformation for different batches of DGI (Figure 2a;[21] Figure 1b inset[22]). Figure 3a,b show the co-surfactant concentration effects on the tensile stress−strain curves. All samples showed overlapped tensile behaviors at small strain (strain <2.5) but the tensile behaviors at large strain (strain >2.5) where strain-hardening starts to occur was highly dependent on the co-surfactant chemical structure and concentration. Before the yielding strain (ca. 0.25), bilayers deform without rupture, while at a large strain, bilayer rupture occurs.[22] Therefore, the effect of the co-surfactant on the self-assembly of bilayers and on their rupture can be elucidated by analyzing the stress−strain curves at small and large strain, respectively.

The small strain behavior is shown in Figure 3a,b as insets. Concentration dependence is observed for both anionic co-surfactants SDS and SST but not for DTAC and NBA as emphasized in semi-log plots in Figure S4. If the elasticity of the hydrogels at small strain is dominated by the inter-lamellar distance, we would expect that the modulus E and interlayer spacing d follow the relation $E \sim 1/d$. However, such correlation is not observed (Figure S5). This result suggests that DGI molecular packing slightly depends on R. To verify this speculation, we calculated the Young modulus of the bilayer from the Young modulus of the PDGI/PAAm hydrogels (Figure S6) and that of the pure PAAm hydrogel. The results of bilayer modulus are shown in Figure 2c. As expected, hydrogels with SST (R = 1:250) that showed lateral swelling have relatively soft PDGI bilayers (1 MPa), while bilayers with DTAC are significantly stiffer (4.8−6.1 MPa). Hydrogels with SDS and NBA exhibit a similar range of bilayer stiffness (2.8−4.7 MPa). Interestingly, when compared at the same hydrophobic tail length (l_t = 12 for SDS and DTAC), it seems that the smaller headgroup area of the co-surfactant induces higher stiffness of the bilayers (DTAC) than the larger headgroup area (SDS). Noticeably, increasing NBA concentration up to R = 1:64 does not further stabilize the bilayer.

At large strain, samples with NBA or DTAC (Figure 3b) showed stronger strain-hardening than samples with SDS or SST (Figure 3a). SDS concentration at R = 1:1000 seemed to enhance strain-hardening, while hydrogels with SST at 1:250 and 1:1000 molar ratio to DGI appeared distinctly softer (see the semi-log plot in Figure S7). Noticeably, the hydrogel with SST at R = 1:1000 exhibited a much higher Young's modulus than that of the hydrogel at R = 1:250 (almost 3 fold), stressing that the behavior at small and large strains originates from different mechanisms. Surprisingly, hydrogels with NBA or DTAC exhibited a concentration-dependent strain-hardening behavior (except for NBA at R = 1:64): strain-hardening was enhanced at higher NBA concentration (R = 1:250) and at lower DTAC concentrations (R = 1:8000) (Figure 3b and Figure S8). Therefore, small changes in co-surfactant concentration dramatically affected the tensile response of PDGI/PAAm hydrogels at small and large strains.

It is worth mentioning that during swelling, PAAm gel layers exert a biaxial tension onto the bilayers because the gel layers intend to swell in an isotropic manner. Consequently, bilayers might become less stable in a hydrogel at the equilibrium swelling state and more susceptible to rupture under tensile deformation. In order to skirt swelling-induced effects, the tensile behavior of the hydrogels was further investigated in their as-prepared state. For comparison purposes, hydrogels with SDS or NBA were chosen as models for each type of mechanical behavior (with R = 1:1000, 1:500, and 1:250). It should be noted that the mechanical behavior of pure PAAm hydrogels without DGI is independent of the presence of SDS or NBA (Figure S9). As plotted in Figure 3c, the tensile response of hydrogels with NBA at the as-prepared state showed weak dependence on its concentration. In contrast, a lower SDS content correlated with enhanced strain-hardening at large strains. Small strain behavior and Young's moduli of the hydrogels increased with decreasing SDS concentration but showed slight inverse dependence on NBA concentration (Figure 3c, inset and Figure S10).

To investigate how swelling affects the mechanical behavior of the hydrogels, we compared samples at the as-prepared and equilibrium swelling states. Since small strain behavior mostly arises from physical interactions within PDGI bilayers, we plotted tensile curves of hydrogels with NBA or SDS at R = 1:500 at the swollen state with correction of the nominal stress by their thickness swelling ratio in Figure 3d (see Figure S11 for a comparison of non-corrected curves). At small deformation (Figure 3d, inset), the tensile behavior at the as-prepared state and corrected swollen state collapsed within experimental error. This indicates that swelling of the PAAm gel layer actually has little effect on the PDGI bilayers. However, at large deformation, there is a significant difference even after correction. This means that the interactions between PAAm gel layers and PDGI bilayers are reduced to a greater extent than what would be expected from the softening induced only by swelling. This result suggests that the hydrogen bonds between PAAm strands and PDGI bilayers are weakened by swelling mismatch.

From the swelling-induced softening at large deformation, we speculate that the chemical structure of the co-surfactant

https://doi.org/10.1021/acsomega.3c02274
ACS Omega 2023, 8, 25185−25194

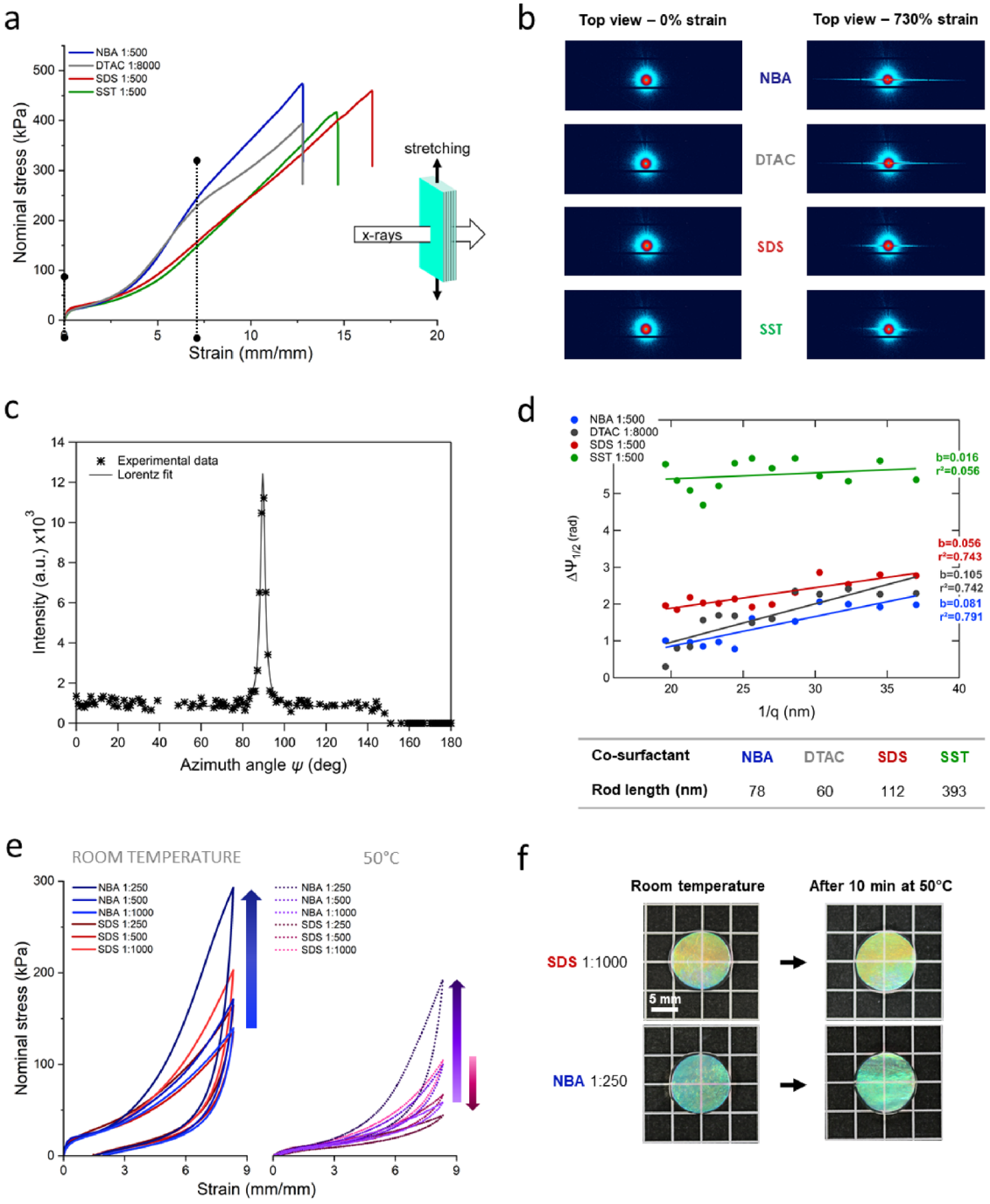

Figure 4. Mechanism of deformation and energy dissipation during tensile loading of PDGI/PAAm hydrogels. (a) Uniaxial tensile behavior of the hydrogels with different co-surfactants compared at fixed R (at similar bilayer stiffness). (b) USAXS patterns correlate with the strain-hardening or softening at large deformation. (c) Ruland's streak method was applied at 730% strain for the hydrogels at fixed R, (d) from which the length of rod-like structures in the different hydrogels was determined. (e) Cyclic tensile behavior at room temperature or 50 °C of PDGI/PAAm hydrogels with either SDS or NBA co-surfactants at different R (swollen at equilibrium). (f) Photos of the photonic hydrogels at different temperatures.

also plays a role in the physical interactions between PAAm gel layers and PDGI bilayers.

Co-surfactant-Dependent Toughening Mechanism at Large Strain in Photonic Hydrogels. Figure 4a compares the large strain tensile behavior of the selected hydrogels at R = 1:500 for SDS, NBA, and SST and R = 1:8000 for DTAC. This concentration was chosen because of similar bilayer stiffness (or highest one in the case of SST). A previous study on PDGI/PAAm hydrogels with the SDS co-surfactant at R = 1:4000 showed that stretching along the direction of the lamellae induces structure transformation to fibrous structures aligned along the deformation axis. The rupture of PDGI bilayers occurred with the formation of rod-like structures at small elongation (strain ~1−4).[22] In order to understand the origin of strain-hardening or softening at large elongation, we performed USAXS to compare the structural changes in the hydrogels with different co-surfactants. To reveal how elongation affects the rupture of the bilayers, we studied the in-plane structure by imposing the X-ray beam perpendicular to the plane of the lamellae (Figure 4a, schematics). The 2D

https://doi.org/10.1021/acsomega.3c02274
ACS Omega 2023, 8, 25185−25194

USAXS patterns of PDGI/PAAm gels are shown in Figure 4b for strain ∼0 and strain ∼7.3, where large differences in strain-hardening behavior were observed for different co-surfactants. At strain ∼0, the 2D patterns showed a very weak and diffuse isotropic scattering, confirming the in-plane isotropic structure of the bilayers independent of the co-surfactant (Figure S12). Such isotropic patterns strongly contrast with the ones observed perpendicular to the bilayers (Figure S13). At strain ∼7.3, the 2D patterns were strongly anisotropic, and two scattering streaks in the equatorial direction were clearly observed perpendicular to the deformation direction. Such streaks have been observed before in tough hydrogels where the structure, initially isotropic, becomes anisotropic during uniaxial stretching (alignment along the stretching direction).[23] In PDGI/PAAm hydrogels, streaks are a characteristic signature of rod-like structures, indicating the rupture of bilayers along the elongation direction.[22] Therefore, rupture of the bilayers and alignment of the PAAm chains along the tensile direction occur simultaneously at large strains.

Interestingly, USAXS patterns at strain ∼7.3 correlate well with the co-surfactant-dependent large-strain tensile behavior. The streaks of hydrogels with NBA or DTAC that showed distinct strain-hardening are much longer than those of SDS and SST, indicating that rod-like structures are relatively shorter for the gels showing strain-hardening. To quantitatively estimate the rod length, we adopted the Ruland streak method.[24] An example of Lorentzian fit of experimental data from the SDS 1:500 sample (integrated profile of the 2D azimuthal plot at q = 2.7 m Å^{-1}) is shown in Figure 4c. Figure 4d shows the Ruland plot, that is, the azimuthal widths, $\Delta\psi_{1/2}$ along the equatorial axis (ψ = 90) against the inverse of scattering vector, $1/q$. The rod length L estimated from the slope of the Ruland plot is shown in the table below the plot. It is worth mentioning that USAXS intensity is weaker than that of SAXS, explaining lower r^2 during line fitting. From these results, we can state that hydrogels with NBA and DTAC have shorter rod-like structures (below 80 nm), while those with SDS and SST have longer ones (112 and 393 nm, respectively). Therefore, we may hypothesize that the breaking of the bilayers into rods shorter than 80 nm efficiently contributes to the strain-hardening behavior of the hydrogel. Indeed, breaking more physical bonds between DGI monomers induces more energy dissipation. Such behavior reminds that of spider-silk under uniaxial tension, where similarly, strain-hardening at large deformations was associated to enhanced H-bond breakage within silk protein β-sheets.[25]

To test this hypothesis, we compared the cyclic tensile behavior of PDGI/PAAm hydrogels with SDS or NBA at large deformation (up to strain ∼8.3). As plotted in Figure 4e (first cycle only), PDGI/PAAm hydrogels with SDS did not exhibit significantly different cyclic behavior nor peak stress with respect to their SDS content. In contrast, hydrogels with NBA reached higher peak stress and larger hysteresis loop with increased NBA content. All PDGI/PAAm hydrogels exhibited larger hysteresis loop during the first cyclic loading and unloading, followed by smaller loops that are almost overlapped in the later cycles (Figure S14). Such behavior is typical of pure physical hydrogels,[26] confirming that energy dissipation processes mostly originate from breaking of non-covalent interactions, like sacrificial bonds. In order to probe the strength of physical interactions, the same set of experiments was conducted at a high temperature (∼50 °C), above the Krafft point of DGI (43 °C), where bilayers are expected to behave like a liquid crystal. First, the Young modulus of all hydrogels dropped by a ∼9 fold factor and did not seem to be influenced by the concentration of co-surfactants (Figure S15). It became close to that of a single PAAm hydrogel, about 10 kPa, confirming that bilayers lost their cohesion at the macroscopic scale. Second, Figure 4f shows that all hydrogels still exhibited bright structural color after heating, indicating that the lamellar organization is preserved at ∼50 °C. Finally, the cyclic tensile behavior (first loop) in Figure 4e shows that hydrogels with increasing NBA content still exhibited higher peak stress at large deformation, while hydrogels with increasing SDS concentration showed opposite trend and lower peak stresses. The hysteresis of the first loop appeared reduced independent of the co-surfactant, suggesting a decrease in the strength of physical interactions. However, the amount of dissipated strain energy at 50 °C during the first cycle is still somewhat preserved at the highest NBA content (Figure S16). At the solution state, it is known that higher temperatures tend to decrease the solubility of amphiphiles due to reduced hydration of the hydrophilic headgroups.[27] As a consequence, headgroup/headgroup repulsion becomes weaker, which decreases their occupied surface area and may change their optimal configuration, that is, from lamellae to inverted micelles in the case of DGI. This phenomenon could reduce the strength of hydrophobic interactions within PDGI bilayers, thus reducing both peak stress and hysteresis at 50 °C. However, the somewhat preserved physical interactions at high temperature and highest NBA concentration reveal the strength of interfacial interactions in this system.

Knowing that PAAm strands were shown to adsorb strongly via hydrogen bonds onto PDGI bilayers,[14] we propose the following mechanism. At the as-prepared state, both the co-surfactant concentration and the chemical structure determine the number of anchorage points between PAAm strands and PDGI bilayers. More specifically, cationic co-surfactants (DTAC and NBA) would tend to promote such physical bonds more than anionic co-surfactants (SDS, SST) due to the affinity of PAAm chains for positively charged surfaces.[28] Since the number of adsorption sites of PAAm strands onto PDGI bilayers was shown to increase with decreasing amounts of water molecules,[15] it is also possible that co-surfactants with a smaller headgroup area than DGI (NBA and DTAC) tend to hydrate DGI headgroups less than SDS or SST, thus promoting PAAm adsorption. After swelling, some of the hydrogen bonds between PAAm strands and PDGI bilayers are irreversibly broken due to swelling mismatch between the bilayer and the PAAm gel layer, independent of the co-surfactant. During uniaxial tensile deformation, the rigid PDGI bilayers carry the load first and then break into rod-like objects of about 800 nm length until strain ∼4.[22] Then, the load is transferred to the soft PAAm gel layers through hydrogen bonding of PAAm strands onto a hard bilayer surface, as reported in another nanocomposite system.[29] PAAm strands with more anchorage points (NBA and DTAC) tend to reach their limit of extensibility at lower strains, thus inducing strain-hardening. Due to strain-hardening of PAAm strands, PDGI bilayers further rupture into smaller rods as strain increases, which dissipates energy. When compared at strain ∼7.3, more adsorption induces stronger strain-hardening. Overall, this mechanism reminds that of double network hydrogels,[30] where physical bonds between the two networks provide synergistic reinforcement mechanisms.[31,32] In the case of hydrogels with

https://doi.org/10.1021/acsomega.3c02274
ACS Omega 2023, 8, 25185−25194

SDS or SST, less anchorage points imply that PAAm strands carry load mostly in the bulk of the PAAm gel layer and PDGI bilayers break into longer rods (less efficient load transfer and lower energy dissipation).

CONCLUSIONS

Self-assembled PDGI/PAAm hydrogels exhibiting structural colors were successfully synthesized in the presence of small amounts of different co-surfactants. Even at such small molar ratios to DGI, the concentration and chemical structure of co-surfactants were found to influence significantly the structure and mechanical behavior of the photonic hydrogels. At small strain, the concentration of co-surfactants was found to impact DGI packing within bilayers, that is, bilayer stiffness but the co-surfactant structure had limited influence. At large strain, the change in bilayer density did not account for large differences in tensile stress between samples at the as-prepared state and equilibrium swelling state. Thus, swelling mismatch between the PAAm gel layer and the bilayers dramatically weakens the adsorption of PAAm strands onto bilayers. PDGI/PAAm hydrogels with neutral or cationic co-surfactants exhibited a pronounced strain-hardening at large deformation, not present with anionic co-surfactants. The strain-hardening correlated with the rupture of bilayers into smaller rods as analyzed by USAXS, which enhances energy dissipation. We hypothesize that, in contrast with anionic co-surfactants, neutral or cationic co-surfactants would promote strong adsorption of PAAm strands onto PDGI bilayers, thus improving load transfer after rupture of the bilayers at large deformation. This study highlights the importance of interfacial interactions in this lamellar bilayer/hydrogel composite system, thus providing clues to the design of tougher photonic hydrogels only by small changes in their composition.

ASSOCIATED CONTENT

Supporting Information

The Supporting Information is available free of charge at https://pubs.acs.org/doi/10.1021/acsomega.3c02274.

Cryo-SEM micrographs, wavelength at maximum reflectance intensity and interlamellar distance, Young's moduli and methodology for calculating bilayer modulus, tensile behavior of PAAm gels with co-surfactants only, Young's moduli of PDGI/PAAm hydrogels at the as-prepared state, and comparison of the tensile behavior of the hydrogels at the as-prepared and equilibrium swelling states (PDF).

AUTHOR INFORMATION

Corresponding Author

Jian Ping Gong − *Laboratory of Soft & Wet Matter (LSW), Faculty of Advanced Life Science and Institute for Chemical Reaction Design and Discovery (WPI-ICReDD), Hokkaido University, Sapporo, Hokkaido 001-0021, Japan;* orcid.org/0000-0003-2228-2750; Email: gong@sci.hokudai.ac.jp

Author

Milena Lama − *Laboratory of Soft & Wet Matter (LSW), Faculty of Advanced Life Science, Hokkaido University, Sapporo, Hokkaido 001-0021, Japan;* orcid.org/0000-0001-8373-6336

Complete contact information is available at: https://pubs.acs.org/10.1021/acsomega.3c02274

Author Contributions

The manuscript was written through contributions of all authors. All authors have given approval to the final version of the manuscript.

Funding

M.L. is the recipient of a JSPS Postdoctoral Fellowship for Research in Japan. This project was funded by a Grant-in-Aid for Scientific Research n°JP21F20769 and JSPS KAKENHI n°JP17H06376, n°JP22H04968, and JP22K21342.

Notes

The authors declare no competing financial interest.

ACKNOWLEDGMENTS

Cryo-SEM observations were performed at the Electron Microscope Laboratory, Research Faculty of Agriculture, Hokkaido University, with the technical support of Dr. Masanori Yasui. Prof. Takayuki Kurokawa is acknowledged for contributing to Spring-8 USAXS proposal and measurements. Dr. Ryuji Kiyama, Mr. Sho Ohmura, Ms. Haruna Tsuchibora, Dr. Xueyu Li, and Dr. Shi Dong are warmly thanked for their help and support during USAXS measurement. Dr. Yanan Ye and Ms. Matsumoto are acknowledged for providing technical training and advice. Dr. Tasuku Nakajima and late Dr. Dan King are thanked for fruitful discussions. Prof. Xiang Li is thanked for his help during USAXS data analysis and interpretation.

REFERENCES

(1) Tiddy, G. J. T. Surfactant-Water Liquid Crystal Phases. *Phys. Rep.* **1980**, *57*, 1−46.

(2) Israelachvili, J. The Science and Applications of Emulsions - an Overview. *Colloids Surf. A: Physicochem. Eng. Asp.* **1994**, *91*, 1−8.

(3) Yamamoto, T.; Satoh, N.; Onda, T.; Tsujii, K. A Novel Iridescent Gel Phase of Surfactant and Order-Disorder Phase Separation Phenomena. *Langmuir* **1996**, *12*, 3143−3150.

(4) Thunig, C.; Hoffmann, H.; Platz, G. Iridescent Colours in Surfactant Solutions. *Prog. Colloid Polym. Sci.* **1989**, *79*, 297−307.

(5) Niu, J.; Wang, D.; Qin, H.; Xiong, X.; Tan, P.; Li, Y.; Liu, R.; Lu, X.; Wu, J.; Zhang, T.; Ni, W.; Jin, J. Novel Polymer-Free Iridescent Lamellar Hydrogel for Two-Dimensional Confined Growth of Ultrathin Gold Membranes. *Nat. Commun.* **2014**, *5*, 3313.

(6) Naitoh, K.; Ishii, Y.; Tsujii, K. Iridescent Phenomena and Polymerization Behaviors of Amphiphilic Monomers in Lamellar Liquid Crystalline Phase. *J. Phys. Chem.* **1991**, *95*, 7915−7918.

(7) Kleman, M. Defects in Liquid Crystals. *Rep. Prog. Phys.* **1989**, *52*, 555−654.

(8) Chen, X.; Mayama, H.; Matsuo, G.; Torimoto, T.; Ohtani, B.; Tsujii, K. Effect of Ionic Surfactants on the Iridescent Color in Lamellar Liquid Crystalline Phase of a Nonionic Surfactant. *J. Colloid Interface Sci.* **2007**, *305*, 308−314.

(9) Ozawa, J.; Matsuo, G.; Kamo, N.; Tsujii, K. Separated Organized Polymerization of an Amphiphilic Monomer and Acrylamide in One-Pot Reaction. *Macromolecules* **2006**, *39*, 7998−8002.

(10) Haque, M. A.; Kamita, G.; Kurokawa, T.; Tsujii, K.; Gong, J. P. Unidirectional Alignment of Lamellar Bilayer in Hydrogel: One-Dimensional Swelling, Anisotropic Modulus, and Stress/Strain Tunable Structural Color. *Adv. Mater.* **2010**, *22*, 5110−5114.

(11) Haque, M. A.; Gong, J. P. Multi-Functions of Hydrogel with Bilayer-Based Lamellar Structure. *React. Funct. Polym.* **2013**, *73*, 929−935.

(12) Haque, M. A.; Mito, K.; Kurokawa, T.; Nakajima, T.; Nonoyama, T.; Ilyas, M.; Gong, J. P. Tough and Variable-Band-Gap

Photonic Hydrogel Displaying Programmable Angle-Dependent Colors. *ACS Omega* **2018**, *3*, 55−62.
(13) Haque, M. A.; Kurokawa, T.; Kamita, G.; Yue, Y.; Gong, J. P. Rapid and Reversible Tuning of Structural Color of a Hydrogel over the Entire Visible Spectrum by Mechanical Stimulation. *Chem. Mater.* **2011**, *23*, 5200−5207.
(14) Li, X.; Kurokawa, T.; Takahashi, R.; Haque, M. A.; Yue, Y.; Nakajima, T.; Gong, J. P. Polymer Adsorbed Bilayer Membranes Form Self-Healing Hydrogels with Tunable Superstructure. *Macromolecules* **2015**, *48*, 2277−2282.
(15) Ilyas, M.; Haque, M. A.; Yue, Y.; Kurokawa, T.; Nakajima, T.; Nonoyama, T.; Gong, J. P. Water-Triggered Ductile-Brittle Transition of Anisotropic Lamellar Hydrogels and Effect of Confinement on Polymer Dynamics. *Macromolecules* **2017**, *50*, 8169−8177.
(16) García-Río, L.; Leis, J. R.; López-Fontán, J. L.; Mejuto, J. C.; Mosquera, V.; Rodríguez-Dafonte, P. Mixed Micelles of Alkylamines and Cetyltrimethylammonium Chloride. *J. Colloid Interface Sci.* **2005**, *289*, 521−529.
(17) Israelachvili, J. N. *Intermolecular and Surface Forces*; Elsevier; 2011.
(18) Corkery, R. W. Langmuir - Blodgett (L - B) Multilayer Films. *Langmuir* **1997**, *13*, 3591−3594.
(19) Haque, M. A.; Kurokawa, T.; Nakajima, T.; Kamita, G.; Gong, J. P.; Fatema, Z. Surfactant Induced Bilayer-Micelle Transition for Emergence of Functions in Anisotropic Hydrogel. *J. Mater. Chem. B* **2022**, *10*, 8386−8397.
(20) Brake, J. M.; Mezera, A. D.; Abbott, N. L. Effect of Surfactant Structure on the Orientation of Liquid Crystals at Aqueous-Liquid Crystal Interfaces. *Langmuir* **2003**, *19*, 6436−6442.
(21) Haque, M. A.; Kurokawa, T.; Kamita, G.; Gong, J. P. Lamellar Bilayers as Reversible Sacrificial Bonds to Toughen Hydrogel: Hysteresis, Self-Recovery, Fatigue Resistance, and Crack Blunting. *Macromolecules* **2011**, *44*, 8916−8924.
(22) Haque, M. A.; Cui, K.; Ilyas, M.; Kurokawa, T.; Marcellan, A.; Brulet, A.; Takahashi, R.; Nakajima, T.; Gong, J. P. Lamellar Bilayer to Fibril Structure Transformation of Tough Photonic Hydrogel under Elongation. *Macromolecules* **2020**, *53*, 4711−4721.
(23) Cui, K.; Sun, T. L.; Liang, X.; Nakajima, K.; Ye, Y. N.; Chen, L.; Kurokawa, T.; Gong, J. P. Multiscale Energy Dissipation Mechanism in Tough and Self-Healing Hydrogels. *Phys. Rev. Lett.* **2018**, *121*, No. 185501.
(24) Perret, R.; Ruland, W. The Microstructure of PAN-Base Carbon Fibres. *J. Appl. Crystallogr.* **1970**, *3*, 525−532.
(25) Du, N.; Yang, Z.; Liu, X. Y.; Li, Y.; Xu, H. Y. Structural Origin of the Strain-Hardening of Spider Silk. *Adv. Funct. Mater.* **2011**, *21*, 772−778.
(26) Lama, M.; Raveendranathan, B.; Brun, J.; Fernandes, F. M.; Boissière, C.; Nassif, N.; Marcellan, A. Biomimetic Tough Gels with Weak Bonds Unravel the Role of Collagen from Fibril to Suprafibrillar Self-Assembly. *Macromol. Biosci.* **2021**, *21*, No. e2000435.
(27) Bock, H.; Gubbins, K. E. Anomalous Temperature Dependence of Surfactant Self-Assembly from Aqueous Solution. *Phys. Rev. Lett.* **2004**, *92*, No. 135701.
(28) Lee, L. T.; Somasundaran, P. Adsorption of Polyacrylamide on Oxide Minerals. *Langmuir* **1989**, *5*, 854−860.
(29) Li, S.-N.; Yu, Z.-R.; Guo, B.-F.; Guo, K.-Y.; Li, Y.-X.; Gong, L.; Zhao, L.; Bae, J.; Tang, L.-C. Nano Energy Environmentally Stable, Mechanically Flexible, Self-Adhesive, and Electrically Conductive Ti 3 C 2 T X MXene Hydrogels for Wide-Temperature Strain Sensing. *Nano Energy* **2021**, *90*, No. 106502.
(30) Gong, J. P. Why Are Double Network Hydrogels so Tough? *Soft Matter* **2010**, *6*, 2583−2590.
(31) Wu, Y.; Qu, J.; Zhang, X.; Ao, K.; Zhou, Z.; Zheng, Z.; Mu, Y.; Wu, X.; Luo, Y.; Feng, S. Biomechanical Energy Harvesters Based On Ionic Conductive Organohydrogels via the Hofmeister Effect and Electrostatic Interaction. *ACS Nano* **2021**, *15*, 13427−13435.
(32) Zhao, Z.; Zhang, L.; Wu, H. Hydro/Organo/Ionogels: " Controllable " Electromagnetic Wave Absorbers. *Adv. Mater.* **2022**, *34*, No. 2205376.

https://doi.org/10.1021/acsomega.3c02274
ACS Omega 2023, 8, 25185−25194